Journal of Medical Systems (2019) 43: 85
https://doi.org/10.1007/s10916-019-1199-3

IMAGE & SIGNAL PROCESSING

Design of Polarization Imaging Detection System for Lung Cancer Cells Based on Microfluidic Chip

Fei Wang[1] · Zhe Zhang[2] · Qixiang Zhong[2] · Zhenglun Yu[2]

Received: 26 December 2018 / Accepted: 3 February 2019 / Published online: 28 February 2019

Abstract

Lung cancer has become an important killer that endangers human health. In order to detect lung cancer cells at an early stage, prevent the proliferation of cancer cells, timely identify and treat cancer cells, a polarization imaging detection system for lung cancer cells based on microfluidic microarray is proposed. The system utilizes the different polarization characteristics of lung cancer cells to detect the polarization of lung cancer cells. Polarization imaging analyzes the pathological changes of biological tissues with imaging polarization degree and polarization difference images, so as to detect the differences between normal areas and pathological areas, and thus detect the differences between normal cells and cancer cells and carry out early treatment and prevention. Therefore, this system design has important research significance in medicine.

Keywords Lung carcinoma cell · Microfluidic chip · Polarization imaging · System design

Introduction

In recent years, the incidence and mortality of lung cancer are increasing gradually, and it has become one of the most dangerous malignant diseases to human life [1]. The increased risk of lung cancer is associated with PM 2.5 and ozone air pollution. Control measures to reduce air pollution may reduce the incidence of lung cancer in the future [2]. Lung cancer is the leading cause of death of all cancers in China. It also has the highest incidence of cancer compared to other cancers. Almost half of all lung cancers occur in people over the age of 70. About 85% of all lung cancers are non-small cell lung cancer (NSCLC) [3]. Most patients have advanced lung cancer. Older patients are at greater risk of chemotherapy toxicity due to unique physiological changes [4]. Palliative care, as a kind of special medical care, is an important treatment method for elderly patients with advanced NSCLC. Low-dose palliative radiotherapy improves respiratory symptoms in elderly patients with NSCLC and has tolerated side effects [5, 6]. Elderly patients with epidermal growth factor receptor (EGFR) mutations benefit from gefitinib and have good tolerance to erlotinib. Cryocare surgical system has an increasing application trend in the treatment of elderly NSCLC patients [7]. Traditional Chinese medicine can improve clinical symptoms, reduce side effects of chemotherapy, and improve the life quality of these patients. Lung cancer is one of the most serious diseases with the highest incidence of NSCLC. The main reason for the failure of chemotherapy is the tolerance to cisplatin. NSCLC is extremely difficult to detect in the early stage of disease. According to statistics, about 70% of patients are not diagnosed with this cancer until the middle and late stage [8]. Therefore, NSCLC has become one of the most harmful diseases to human beings due to its high morbidity, high mortality and low diagnostic rate. However, if the early symptoms of lung cancer can be predicted in advance and timely treatment, then the probability of successful treatment will be greatly improved. In conclusion, in order to reduce the incidence of lung cancer, and to be able to timely diagnosis of lung cancer is a major medical field needs to overcome a major problem. In conclusion, reducing the incidence of lung cancer is a major problem that needs to be solved in the current medical field.

Optical technology has been developing rapidly since the 1960s. Human eyes are more sensitive to the brightness and

✉ Zhenglun Yu
yuzhenglun5915@126.com

[1] Department of Otolaryngology, The First Hospital Affiliated China Medical University, No. 155 Nanjing Street, Heping District, Shenyang 110001, Liaoning Province, China

[2] Department of Thoracic Surgery, The First Hospital Affiliated China Medical University, No. 155 Nanjing Street, Heping District, Shenyang 110001, Liaoning Province, China

color of light, so people have a deep understanding of light intensity and light color in daily life. The phase information of light can't be directly observed, the phase information of light can be obtained through the properties of light diffraction and interference. However, compared with the other three characteristics, people have a shallow understanding of the polarization characteristics of light, there is less research on polarized light, and the application range is small. According to the requirement of bionic polarization navigation for sky polarization mode, a polarization imaging system based on 180° field of view fisheye lens is designed to collect sky polarization information [9]. In addition, the two-dimensional plane polarization mode collected can be restored to the spatial polarization mode through Matlab software. The experimental instrument is calibrated, the imaging formula and parameters of fisheye lens are obtained, and the images collected by polarization imaging system are corrected in the field of observation. Through the calibration system, the corrected spatial polarization mode is consistent with the single Rayleigh scattering theoretical model. They have a high degree of similarity, with an azimuthal polarizability of 82.4% and a polarization similarity of 96.91%. Therefore, polarization technology has not developed as fast as other features. However, due to the rapid development of science and technology, polarization research is attracting more and more interest.

Aiming at the shortcomings of the above status quo, combined with cell detection, polarization imaging detection and microfluidic control technology, and by means of polarization analysis methods such as Mueller matrix, a polarization imaging analysis method based on cell level is proposed. The cells are photographed by a microscope to obtain a set of images in the polarization state, and the polarization characteristics and texture characteristics of the images are analyzed with an image processing algorithm, and the processed polarization data is stored in a database for subsequent research. The system has the characteristics of simple operation, no damage, and no cells marking.

Methodology

Principle and representation of polarization imaging

Maxwell's electromagnetic theory proved that light is a shear wave, and its vibration direction is perpendicular to the propagation direction. Whether the light is polarized or not can be distinguished by the track of the electric field vector E of the light. If the track of E has certain laws, it is completely polarized; if the electric field vector E changes randomly, it is polarized. Light in nature belongs to natural light. In the process of propagation, it will vibrate in all directions perpendicular to the direction of propagation. However, when such light passes through the polaroid, it can only pass in one direction to form polarized light. Due to the birefringence property of the material such as calcite in nature, when natural light is incident on this material, two kinds of light in different directions perpendicular to each other are generated, and one conforms to the general rule of refraction, which is called ordinary light, that is, O-light, and the other, which does not conform to the general rule of refraction, is called extraordinary light, that is, E-light. Therefore, when a beam of light passes through this object with birefringence characteristics, two refringence lights will appear. The schematic diagram of birefringence imaging is shown in Fig. 1. In the figure, the cylinder represents the light source of natural light, whose vibration direction is random, and the ellipse represents the polarizer, after the light passes through the polarizer, its vibration direction can only propagate along a single vibration direction, and the cuboid in the middle represents the object. Due to the extraordinary light generated when light passes through the object, the vibration direction of this light is perpendicular to that of the ordinary light. Therefore, when light passes through the polarizer, it has a component perpendicular to the polarization direction of the polarizer, and eventually the emergent light is emitted.

This principle can be used to determine whether some substances are birefringent or not. In addition to calcite and other substances, the internal structure of some biological tissues and cells also has certain polarization characteristics. In order to quantitatively analyze the polarization characteristics of cells, a formula is needed to fully describe polarized light.

In 1852, Stokes proposed four parameters with light intensity properties to represent different polarization states of light, and formed a set of vectors, which are Stokes vectors. This vector characterization method is convenient to measure, simple to calculate and is the most commonly used method to describe the polarization state of light. To better describe the polarization characteristics of light, Stokes vector method uses four parameters to describe the intensity of light in different directions and in different states. The expression is shown in formula (1).

$$S = \begin{bmatrix} I \\ Q \\ U \\ V \end{bmatrix} = \begin{bmatrix} E_x^2 + E_y^2 \\ E_x^2 - E_y^2 \\ 2E_xE_y\cos\sigma \\ 2E_xE_y\sin\sigma \end{bmatrix} = \begin{bmatrix} I_x + I_y \\ I_x - I_y \\ I_{+45^\circ} - I_{-45^\circ} \\ I_R - I_L \end{bmatrix} \quad (1)$$

In the formula, I, Q, U, and V collectively represent the state of polarized light, which represent total light intensity, linearly polarized light component in the x-axis direction, linearly polarized light component in the 45° direction, and circularly polarized light component, respectively. Among them, E_x and E_y respectively represent the amplitude of the electric field in the X and Y directions, and σ represents the phase difference. I_x, I_y, $I_{+45°}$, $I_{-45°}$, I_R, and I_L indicate light intensities in respective directions. In this way, the polarization state of light can be represented by Stokes vector. Table 1 describes several special Stokes vectors of light in different polarization states.

Fig. 1 Birefringence principle

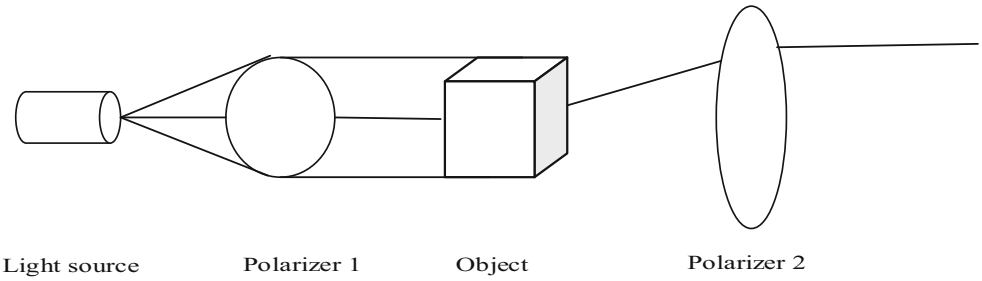

According to Stokes parameters, some polarization parameters can be obtained, such as polarization degree and polarization angle. In this study, the polarization degree parameter is mainly studied. The expression of polarization degree is shown in formula (2).

$$P = \sqrt{\frac{Q^2 + U^2 + I^2}{I}} \tag{2}$$

On the expression of polarized light, compared with Jones vector, the Stokes can better describe completely polarized light, partially polarized light and natural light, and the presentations of Stokes are applicable to all types of light, and four parameters for characterization of light can be directly measured, so many researchers are currently using the Stokes vector method to represent the polarization state of the light.

Decomposition and transformation of Mueller matrix

Since Stokes vector can represent the polarization characteristics of light, Stokes vector can be used to express the incident light and the emergent light generated after it enters the polarization device. Let the Stokes vector of the incident light be S, and the Stokes vector of the emergent light be S'M, representing the material passing by. Both S′ and S are 4*1 matrixes, so the relationship between the incident light, the emergent light and the material passing by is shown in formula (3).

$$S^{'} = MS \tag{3}$$

Table 1 Several special Stokes vector parameters

Special Stokes Vector	I	Q	U	V
Horizontal linear polarization	1	1	0	0
Vertical linear polarization	1	−1	0	0
45 degree linear polarization	1	0	1	0
Negative 45 degree linear polarization	1	0	−1	0
Right circular polarization	1	0	0	1
Left circular polarization	1	0	0	−1
Natural light	1	0	0	0

Formula (3) is expressed in matrix form, and the result is shown in formula (4).

$$\begin{bmatrix} S_1^{'} \\ S_2^{'} \\ S_3^{'} \\ S_4^{'} \end{bmatrix} = \begin{bmatrix} m_{11} & m_{12} & m_{13} & m_{14} \\ m_{21} & m_{22} & m_{23} & m_{24} \\ m_{31} & m_{32} & m_{33} & m_{34} \\ m_{41} & m_{42} & m_{43} & m_{44} \end{bmatrix} \begin{bmatrix} S_1 \\ S_2 \\ S_3 \\ S_4 \end{bmatrix} \tag{4}$$

According to the calculated result, the M matrix is a 4 × 4 matrix, which can characterize the polarization property between the incident light and the emergent light, that is, the light passing through the substance. The 4*4 matrix is the Mueller matrix, which was first proposed by Hans-Mueller in the 1940s. In biology, the microstructures of tissues and cells have a lot of polarization information. To obtain this information, the polarization characteristics of the target need to be expressed with the Mueller matrix. At present, the Mueller matrix can well reflect the polarization characteristics of the target object, and most polarization studies are based on the Mueller matrix. When the incident light passes through the target medium, the polarization state of the emergent light will change. The Mueller matrix is shown in formula (5).

$$M = \begin{bmatrix} m_{11} & m_{12} & m_{13} & m_{14} \\ m_{21} & m_{22} & m_{23} & m_{24} \\ m_{31} & m_{32} & m_{33} & m_{34} \\ m_{41} & m_{42} & m_{43} & m_{44} \end{bmatrix} \tag{5}$$

There is a large amount of polarization information in the parameters of the Mueller matrix, so the Mueller matrix is widely used in the field of polarization characteristic analysis. Many polarization characteristic parameters are realized based on the calculation of Mueller matrix. Therefore, to study the polarization characteristic of the target, it is necessary to obtain each element of the Mueller matrix and conduct further research on this basis.

Gray-level co-occurrence matrix

Due to the complex internal structure of the cell, the gray level of the image can be used to describe the texture of the cell surface structure in the captured image, so the commonly used texture analysis method can be used. In general, it is considered that the pattern formed by the gray value distribution in

the image is considered as texture, that is, the spatial correlation property of the texture, and there may be some gray correlation between two pixel points. Gray-level co-occurrence matrix was first proposed by Haraiick et al. in 1973. It describes texture features by studying the spatial characteristics of gray scale (Fig. 2). Gray-level co-occurrence matrix is widely used in image segmentation of synthetic aperture radar (SAR). In this study, texture characteristics of gray-level co-occurrence matrix under cell polarization state are analyzed and studied.

When all points are counted, the total number of occurrence of all pairs of gray value is calculated and normalized, so that the probability of occurrence of each pair of gray value P (g_l, g_2) can be obtained, and the formula is shown in (6). Among them, R represents the total number of gray value pairs in the gray-level co-occurrence matrix.

$$P(g1, g2) = \frac{p(g1, g2)}{R} \tag{6}$$

There are also differences in size, morphology, and internal structure of cells of the same type, so that some differences in the grayscale texture of the cells are also observed when the image is taken. Therefore, even if it is the same kind of cell, its corresponding gray-level co-occurrence is greatly different. The characteristics of images with different textures are also different. For example, when the texture in the image is fine, its scale has small details, while for the image with coarse texture, its grayscale is smooth, its texture scale is large, and the similar area is large. The gray value of any two pixels in the coarse texture image is close to and concentrated, and the number of elements near the main diagonal of the corresponding gray-level co-occurrence matrix is more than the number of elements in other positions. For the image with smooth fine texture, the gray value of the image changes rapidly in spatial position, the distribution of gray value is scattered, and the corresponding matrix elements are mostly scattered everywhere.

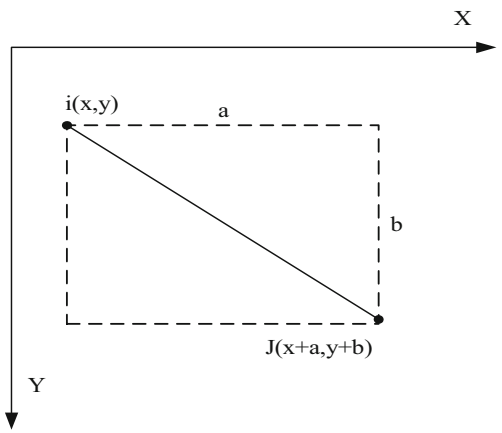

Fig. 2 Principle of gray-level co-occurrence

Results and discussion

Overall design and analysis of polarization imaging detection system for lung cancer cells

The overall structure designed according to polarization imaging theory is shown in Fig. 3. The system structure mainly includes four parts: imaging module, polarization module, image processing module and data module.

This system uses the polarization imaging principle and microfluidic chip technology to analyze the polarization characteristics of cells, so as to identify different cells. Through the imaging module, the cells are photographed under polarized light and the images are displayed in the PC. Due to the differences in the internal structure of cells, the imaging of cells after it passes through polarized light will be different. The cell images taken after passing through polarized light have a large amount of polarization information. Finally, different polarization parameters are extracted with image processing, and the

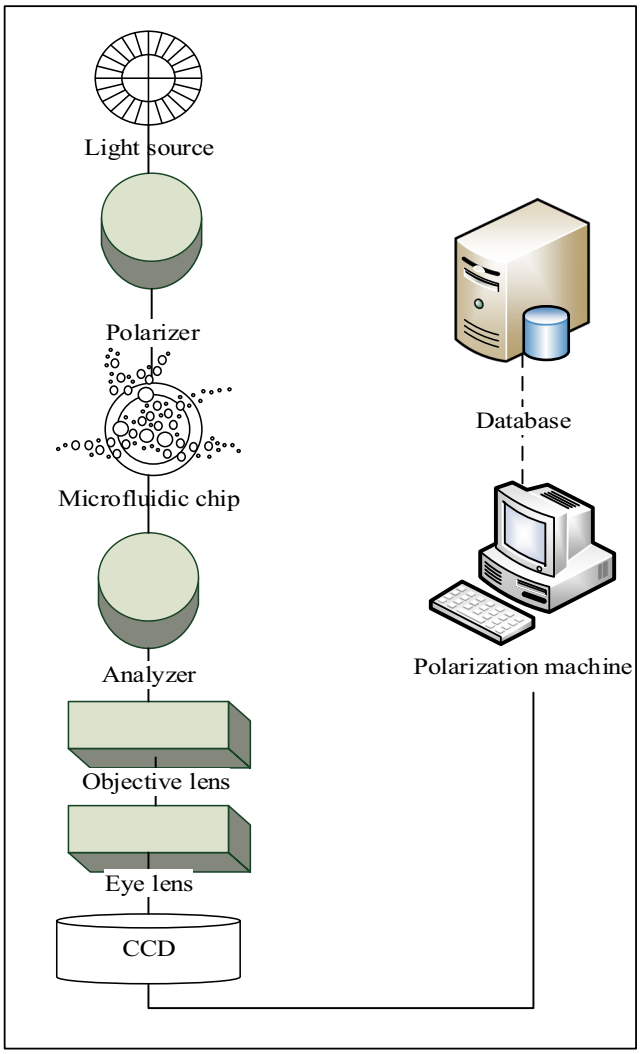

Fig. 3 The overall design framework of the system

polarization parameter images, frequency domain characteristics and texture characteristics of the cells are obtained, so as to realize the recognition of lung cancer cells.

The imaging module in the system is used to amplify the cells. Due to the small size of cells, they need to be magnified to a certain extent to be able to observe the internal structure of cells; the polarization module is mainly composed of the polarizer and the mechanical structure used to fix the polarizer. Its function is to change the natural light emitted by the light source into polarized light. The polarized light changes the polarization direction after passing through the cell sample, so as to characterize the polarization information of the cell; the image processing module stores the captured cells into a PC and uses MATLAB software platform to analyze the polarization characteristics of the image, and obtains different polarization parameters of the cells, so as to compare and analyze a variety of cells; and the function of the database module is to store polarization information processed by the image processing module in the database for subsequent statistical analysis.

The workflow of the whole system is as follows: firstly, the mechanical structure is placed on the objective table of the microscope, and the polarizer is placed on the upper and lower ends of the mechanical structure respectively. The prepared microfluidic chip is placed in the chip groove between the two polarizers. Then, the cell sample is added to one side of the chip, and a small amount of buffer is added to the other side to stabilize the cell sample rapidly. After the sample solution is stabilized, the polarizer and the analyzer are respectively rotated. Since the angle of the polarizer and analyzer changes, the field of vision will also change accordingly. The image of the cells at different polarization angles is captured while rotating the polarizer and the analyzer, and the captured image is stored in the PC through the Charge Coupled Device (CCD) of the microscope. After the PC receives the cell images, the polarization characteristics of the cell images are analyzed by MATLAB program in the PC. Firstly, the location of the cell on the image is extracted, and the Mueller matrix image of the cell is obtained after calculation. Then, the polarization parameter images of the cell are obtained, such as polarization degree image, polarization difference image, Mueller matrix transformation parameter image, and the amplitude spectrum and phase spectrum images in the frequency domain. At the same time, the texture characteristics of cells are separated, and some statistical parameters of gray-level co-occurrence matrix, such as entropy, energy, deficit distance and autocorrelation, are used to analyze the cells, so as to obtain the statistical parameters of texture under different cells. Finally, MySQL is used to build a database to store the polarization information

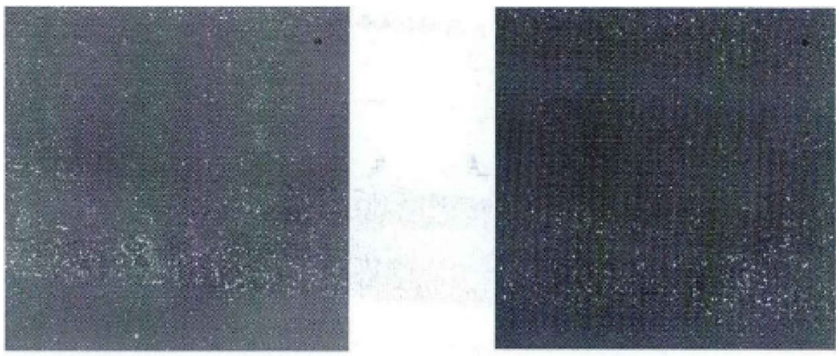

(a) The angle of the polarizer is 0° and 45°

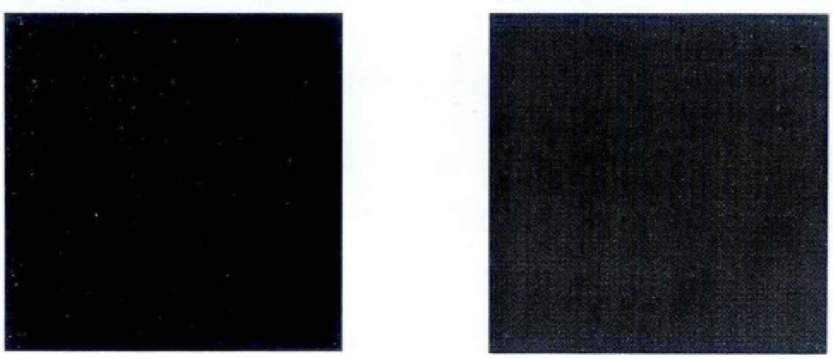

(b) The angle of the polarizer is 90° and 135°

Fig. 4 The results of background measurement

parameters mentioned above, and the database can be retrieved through the program, which is conducive to subsequent analysis and statistics.

Considering that when the sample is actually dropped, if the sample is directly dropped onto the cover glass, the liquid sample will be affected by gravity and move, which will cause the target cells in the sample to move irregularly. The drops also have a certain height so that cells on the same level can't be observed. Therefore, in view of the above shortcomings, microfluidic chip is used as the carrier of cell samples for detection.

Analysis of polarization imaging system for lung cancer cells

In order to evaluate the experimental device, it is necessary to test the device itself. After adjusting the device, turn on the microscope light source and conduct error test on the system. As shown in the figure below, the background is taken and measured before the sample is taken. The background measurement of this experiment means that no samples are put into the objective table for testing, that is, the Mueller matrix of air is solved. In an ideal state, the Mueller matrix of air is shown in formula (7).

$$M = \begin{bmatrix} 1 & 0 & 0 \\ 0 & 1 & 0 \\ 0 & 0 & 1 \end{bmatrix} \tag{7}$$

The relative angles of the two polarizing plates are sequentially adjusted to 0°, 45°, 90°, and 135°, and the results are shown in Fig. 4.

It can be concluded from the figure that the field of view is the brightest at 0°, 45° and 135° are darker than 0°, and the field of view is the darkest at 90°. According to the Mueller solution formula above, the rotation angle of the polarizer is adjusted to take the image, and the result calculated by the program algorithm is shown in formula (8).

$$M = \begin{bmatrix} 1.0000 & -0.0584 & 0.0300 \\ 0.0584 & 1.0000 & 0.0452 \\ -0.1291 & 0.0167 & 0.9821 \end{bmatrix} \tag{8}$$

At the same time, the frequency domain characteristics of polarization microscopic image can be analyzed. Firstly, the

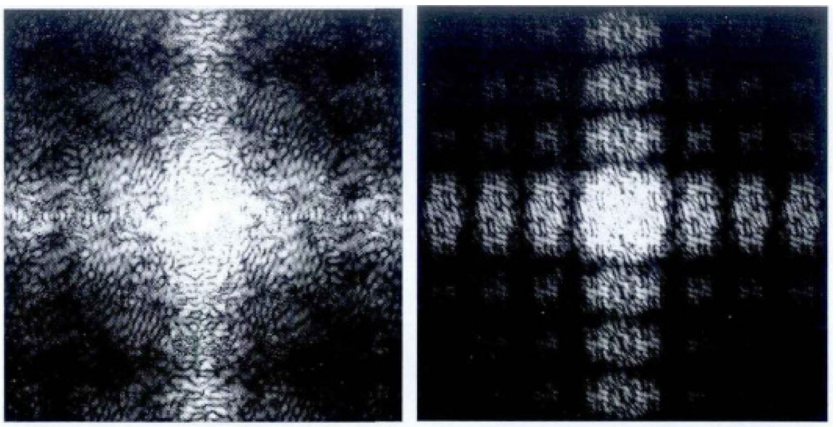

(a) Granule and lung cell CAF

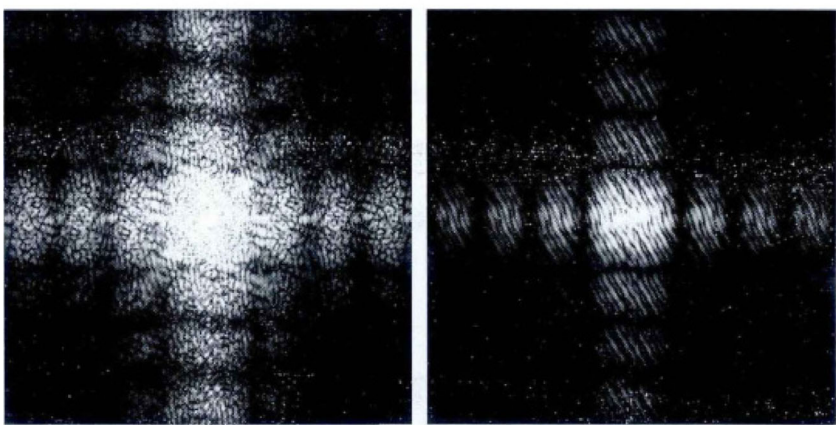

(b) Lung cancer cell A549 and H322

Fig. 5 Polarization difference spectrum image of four kinds of cells

fast Fourier transform is carried out for the polarization difference and polarization degree images of several samples. The fast Fourier transform results under the polarization difference images of four kinds of cells are mainly described. The polarization degree spectrum images are obtained, as shown in Fig. 5. It can be concluded from the figure that the frequency domain characteristics of the four samples are different, and the differences between the four samples are obvious qualitatively. Therefore, it is necessary to further extract the frequency domain characteristics of the polarization images of the amplitude spectrum and phase spectrum images.

The amplitude spectrum images of polarization difference images of four samples are analyzed and their average energy is calculated. The average energy curve of amplitude spectrum of each sample obtained through calculation is shown in Fig. 6. The abscissa represents the sampling point, and the ordinate represents the relative intensity of the spectrum. From the analysis of the average energy curve of the amplitude spectrum, it can be concluded that the average energy curve of the four samples has a main peak at the center, and then gradually decays to both sides. Among them, three kinds of cells have three lateral peaks symmetrically distributed on both sides of the central main peak, and the peak of the lateral peak shows a decreasing trend. According to Fig. 5, the average energy value of particle amplitude spectrum is the highest. The average energy of lung cancer cells A549 is higher than that of lung cancer cells H322, and the average energy of CAF is between the average energy of A549 cells and H322 cells., that is, the particle > A549 > CAF > H322. According to the image, when the x-coordinate value is fixed, the trend of several samples is consistent. Therefore, the average energy curve of polarization degree amplitude spectrum can clearly distinguish the amplitude characteristics of the frequency domain of three kinds of cell polarization microscopic images.

The phase average zero crossing rate (ZCR) can represent its phase change. At a sampling point, the higher the average zero crossing rate is, the more drastic the phase change of the image around this point is; otherwise, the slower the phase change is. According to the calculation results of the mean and variance of the average zero-crossing rate of the four samples, the mean and variance of the average zero-crossing rate curve of the phase spectrum of the polarization difference image of the four samples are obtained, as shown in Table 2. As shown in the table, the average zero crossing rate curve of phase spectrum between polystyrene particles and the three kinds of cells is different. The average zero crossing rate and variance values of the four samples are shown in the following

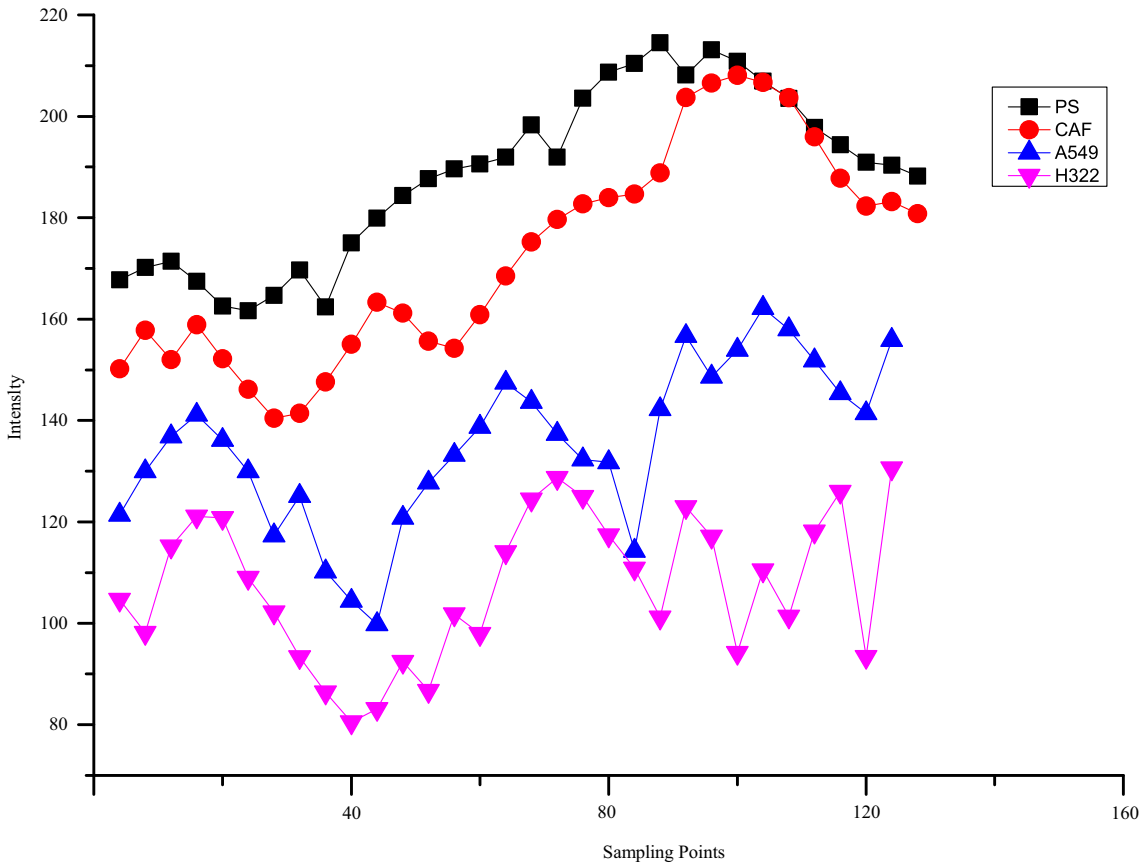

Fig. 6 DP amplitude image average energy curve

Table 2 The mean and variance of the average zero crossing rate of the four samples

Sample Type	Mean	variance
Polystyrene Granule	8.6364	1.8202
CAF	10.8701	1.8592
A549	8.2727	2.6835
H322	9.9740	2.0195

table. According to the results, the mean value of fibroblast CAF is large, and the variance value of cancer cells A549 and H322 is large, which can be used as a reference for cell differentiation.

The four texture variation parameters mentioned above are calculated respectively to characterize the texture characteristics of the cell polarization difference image. The calculation results are summarized as follows: among the four samples, the difference between entropy parameter and parameter autocorrelation is the most obvious. Among the entropy parameters, the particles are significantly lower than those of the three cells. Because the internal structure of the particles is uniform, there is a small uncertainty, that is, the entropy value is lower; among the three types of cells, the entropy value of fibroblasts is higher than that of lung cancer cells A549 and H322, which may be due to the fiber structure of fibroblasts is relatively complex, and the texture change is relatively obvious; lung cancer cell A549 have higher entropy value than H322; among the deficit distance parameters, the deficit distance parameter of particles is the smallest, indicating that the homogeneity of particles is low and local texture changes are small. Among the three types of cells, the deficit distance of A549 cells is the largest and the deficit distance of H322 cells is the smallest, respectively corresponding to the local texture change degree of the internal pair of cells; in the autocorrelation parameters, the particle is significantly lower than the three types of cells. Similarly, the internal structure of particle is uniform, so it has a higher autocorrelation; for autocorrelation in cells, CAF < A549 < H322, the texture consistency of fibroblast CAF polarization difference images is the weakest, and the texture consistency of lung cancer cells H322 is higher than that of A549.

Conclusion

Polarization imaging method can effectively suppress the scattered photons in the deep layer of biological tissue, so as to improve the contrast of imaging. According to the research, polarization imaging method is very suitable for the diagnosis and detection of biological tissue lesions. Polarization imaging technology is unique in optical imaging method due to its unique advantages in the field of biomedicine. This method can influence polarized light through the microstructure inside the organization, so as to obtain a large amount of polarization information, which can enhance the contrast of imaging and reflect the results in the form of imaging for further analysis. Therefore, the polarization imaging detection system of lung cancer cells based on microfluidic chip plays a very important role in the field of biomedicine.

Compliance with ethical standards

Conflict of interest Author Fei Wang declares that he has no conflict of interest. Author Zhe Zhang declares that he has no conflict of interest. Author Qixiang Zhong declares that he has no conflict of interest. Author Zhenglun Yu declares that he has no conflict of interest.

Ethical approval All procedures performed in studies involving human participants were in accordance with the ethical standards of the institutional and/or national research committee and with the 1964 Helsinki declaration and its later amendments or comparable ethical standards.

This article does not contain any studies with animals performed by any of the authors.

Informed consent Informed consent was obtained from all individual participants included in the study.

Publisher's Note Springer Nature remains neutral with regard to jurisdictional claims in published maps and institutional affiliations.

References

1. Zhang, Y., Elgizouli, M., Schöttker, B., Holleczek, B., Nieters, A., and Brenner, H., Smoking-associated dna methylation markers predict lung cancer incidence. Clin. Epigenetics 8(1):127, 2016.
2. Jiang, S., and Li, P., Progress in Palliative Care Benefit of Elderly Patients with Non-small Cell Lung Cancer. Chinese Journal of Lung Cancer 18(7):462, 2015.
3. Li, W., Liu, X., Zhang, G. Q. et al., Role of SOX4 on DDP resistance in non-small cell lung cancer cell of A549. Zhongguo fei ai za zhi = Chinese Journal of Lung Cancer 20(5):298–302, 2017.
4. Ding, Z., Liang, C. P., and Chen, Y., Technology developments and biomedical applications of polarization-sensitive optical coherence tomography. Frontiers of Optoelectronics 8(2):128–140, 2015.
5. Yoo, M., Kim, H. K., and Lim, S., Angular- and Polarization-Insensitive Metamaterial Absorber Using Subwavelength Unit Cell in Multilayer Technology. IEEE Antennas & Wireless Propagation Letters 15:414–417, 2016.
6. Guo, C., Liu, F., Chen, S. et al., Advances on Exploiting Polarization in Wireless Communications: Channels, Technologies, and Applications. IEEE Communications Surveys & Tutorials 99:1–1, 2016.
7. Xiao, D., Yi-Hua, H. U., Nan-Xiang, Z. et al., Research on polarization diversity technology in coherent differential absorption lidar. Journal of Optoelectronics·Laser 26(3):541–547, 2015.
8. Gouget, C. L. M., Hwang, Y., and Barakat, A. I., Model of cellular mechanotransduction via actin stress fibers. Biomech. Model. Mechanobiol. 15(2):1–14, 2016.
9. Fernandez, R. E., Rohani, A., Farmehini, V., and Swami, N. S., Review: microbial analysis in dielectrophoretic microfluidic systems. Anal. Chim. Acta 966:11–33, 2017.